Available online at www.sciencedirect.com

ScienceDirect

Procedia Engineering 171 (2017) 821 – 835

Procedia Engineering

www.elsevier.com/locate/procedia

Sustainable Civil Engineering Structures and Construction Materials, SCESCM 2016

Numerical analysis of RC columns accompanied with friction damping mechanism under cyclic loading

Angga Fajar Setiawan[a,*], Yoshikazu Takahashi[a], Junji Kiyono[a], Sumio Sawada[a]

[a]*Kyoto University, Kyoto, Japan*

Abstract

This paper explains about numerical analysis of RC column accompanied with friction damping mechanism (FDM) under cyclic loading based on the previous experiment. This is new structure system contains three parts of concrete column connected with friction devices together PC bolts confinement. The experiment was performed with cyclic loading test in some variations of PC bolts confinement distribution scenario. In this study non-linear finite element analysis is performed by modeling the column with fiber section element and the friction devices with two-node-link-element. The important parameter in this study is constitutive material of friction devices, concrete, and steel. The hysteresis curves comparison between experiment and numerical results show that the peak forces in the every last loops and hysteresis curves shape characteristics have similarity as well as on the main stiffness and the distributions of moment curvature patterns. The force and displacement monitoring are useful to know the confinement distribution role the slip distribution to each friction devices.

Peer-review under responsibility of the organizing committee of SCESCM 2016.

Keywords: RC Column; Friction Damping Mechanism; Cyclic Loading; Elastic-Plastic Behavior; Numerical Analysis

1. Introduction

The modern seismic design principle concept is the structure shall secure the seismic performance. The structure shall be designed to localize limited damage and to prevent collapse against strong seismic motions. In the level small earthquake that highly probable to occur during the service period the structure has elastic behavior, the

* Corresponding author. Tel.: +81-75-383-3249; fax: +81-75-383-3253.
E-mail address: angga.setiawan.85z@st.kyoto-u.ac.jp

Peer-review under responsibility of the organizing committee of SCESCM 2016.
doi:10.1016/j.proeng.2017.01.373

otherwise in the level severe earthquake that less probable to occur during service period it was allowed have inelastic behavior, but limit damaged.

The previous study was done by performing experiment of high seismic-performance column under cyclic loading [1-3]. This is new structure system contains three parts of concrete column connected with friction device together PC bolts confinements, the illustration can be seen at Fig. 1. Based on the experiment result this structure has large enough elastic deformation with sufficient energy dissipation. The maximum elastic drift ratio is about 2% and the restoring force is fairly constant up to 10% drift.

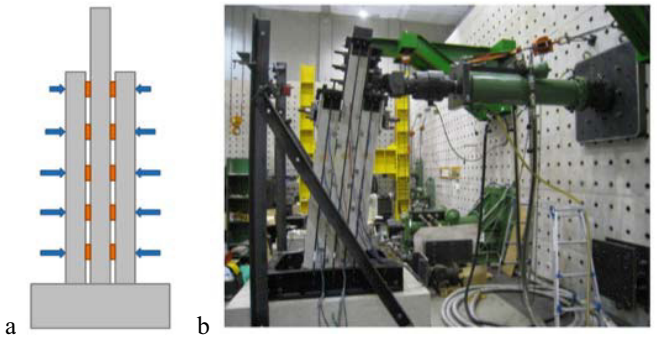

Fig. 1. (a) The column accompanied with FDM illustration; (b) experiment of column accompanied with FDM under cyclic loading [1].

2. Column accompanied with friction damping mechanism

2.1. Friction device characteristic

The friction device follows the Coulomb dry friction law, friction force in both condition starting slip (static friction) and slip (kinematic friction) to be assumed constant value due to subjected low pressure and high enough to produce excessive deformation with low relative velocity [4]. The friction coefficient (μ) can be determined as:

$$\mu = \frac{|F_{\max}|}{N} \tag{1}$$

Nakamura [3] conducted experiment of friction devices testing, that contain friction material of steel type SS400 accompanied with steel type SUS304 as the couple. This experiment result showed that the friction coefficient value increase almost linear with slip increment, start from about 0.2 at first slip until about 0.5 in the end of loading, the force and displacement curve of FDM can be seen at Fig. 2.

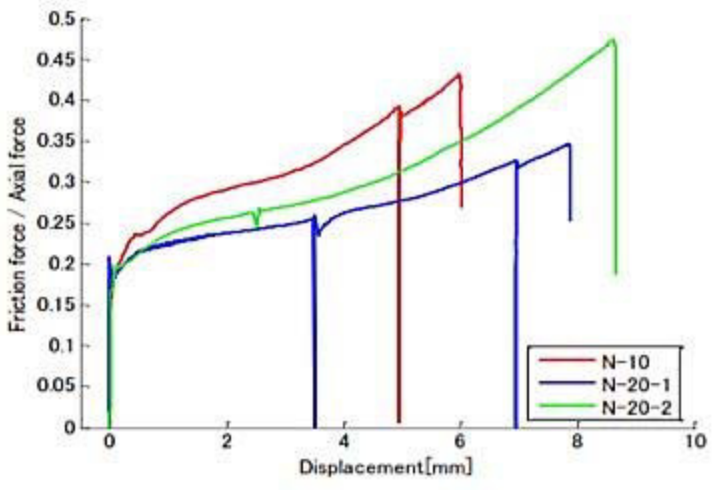

Fig. 2. Friction coefficient from monotonic loading test [5].

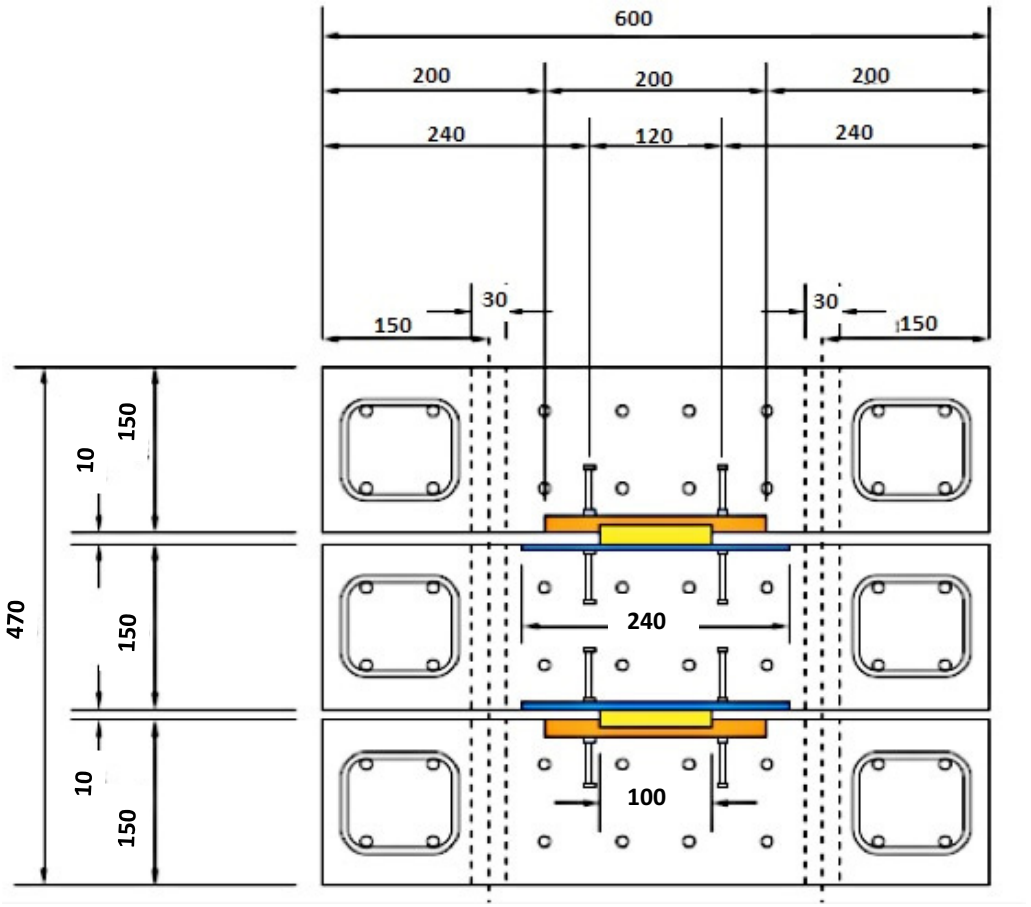

Fig. 3. Column section with FDM configuration [1].

2.2. The column accompanied with friction damping mechanism specimen properties

The structure system contains three parts of concrete column with fix support at the base and free constraint at top location. The three parts of column configuration to be connected with friction device and PC bolts to give confinement effect to those at every 300 mm intervals in 1500 mm of the column height. The concrete column section has 600 mm of width and 150 mm of depth, contains 16D10 longitudinal reinforcement bars and 2D6 with 50 mm spacing transversal reinforcement, the illustration can be seen at Fig. 3. The concrete compressive strength of column specimen is 37 MPa, the longitudinal reinforcement steel type is SD345, and the transversal reinforcement steel type is SD295.

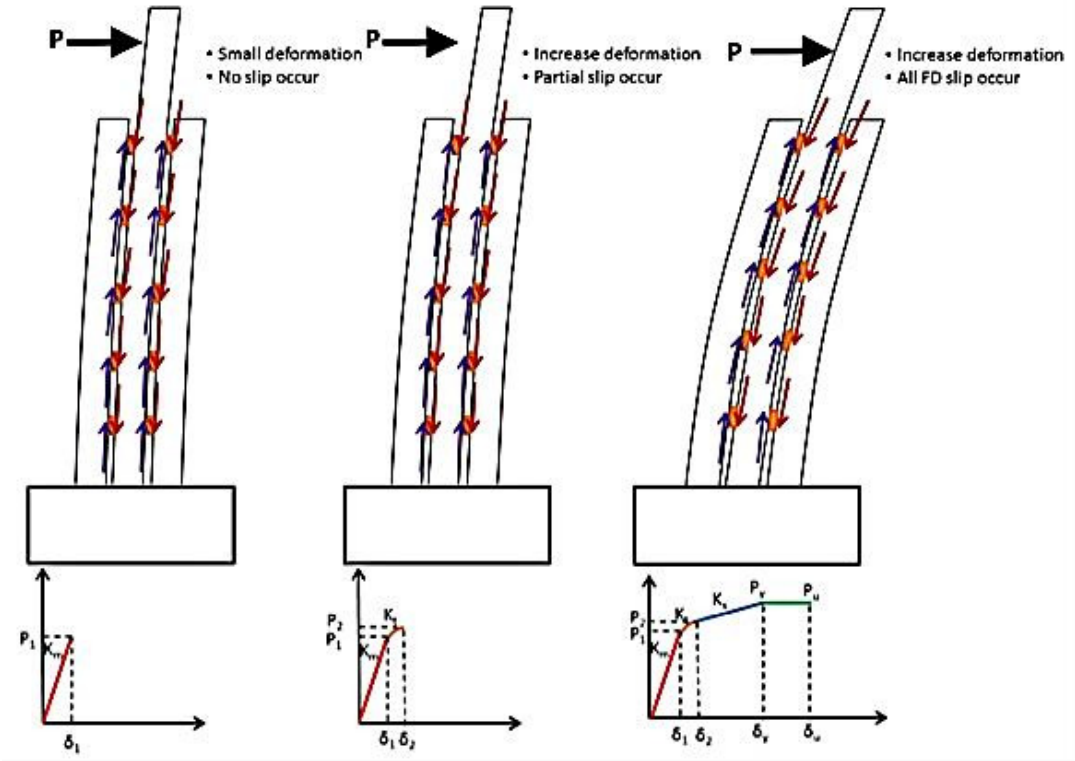

Fig. 4. The skeleton curve characteristic of column accompanied with FDM.

2.3. The structure accompanied with FDM behavior

The principle of the column accompanied with friction damping mechanism is to achieve large enough elastic deformation by dividing the rectangular column section in the several rectangular columns, while friction devices connect the column components with horizontal confining forces of PC bolts provide energy dissipation when slip deformation occurs in case lateral deformation [6]. When small the lateral force (P) works to the top of column, small lateral deformation is formed, slip has not yet occurred on the friction devices, the stiffness of the column is K_m (monolith stiffness). The other hand the larger lateral force (P) the larger deformation to the column, slip occurs at some part of friction devices, the stiffness of the column decrease to be K_t (transition stiffness), and then along with increased lateral deformation slip occur at all friction devices, the stiffness to be K_s (separated stiffness) which is the smallest stiffness. This mechanism produces energy dissipation in the elastic up to plastic behavior, the illustration can be seen in the Fig. 4.

3. The experiment of column accompanied with friction damping mechanism

The main focus of the experiment is to investigate the influence of FDM confinement distribution to obtain the behavior of this structural system. There are two kinds of specimen that to be tested, the specimen number 1 to be confined by two PC bolts in the outer location of FDM, however the specimen number 2 to be confined by one PC bolt in the center location of FDM. There are four distribution variations of FDM confinement in those specimens, which can be seen at Table 1.

Seven variations of cyclic loading scenario were performed that can be seen at Table 2. All cyclic loading scenarios used specimen number 1 except the scenario T20-3 that used specimen number 2. In this experiment the cyclic loading test implemented displacement control.

Table 1.Confinement force configurations.

Elevation (mm)	Confinement force (Tonf)			
	U10	T10	T20	T40
300	10.0	10.0	20.0	40.0
600	10.0	7.5	15.0	30.0
900	10.0	5.0	10.0	20.0
1200	10.0	2.5	5.0	10.0
1500	5.0	0.0	0.0	0.0

Table 2.Cyclic loading scenarios.

No	Scenario	δ_{max} (mm)
1	U10	-9 to 9
2	T10	-7 to 7
3	T20	-8 to 8
4	U10-2	-17.5 to 17.5
5	T20-2	-17.5 to 17.5
6	T20-3	-200 to 200
7	T40	-160 to 200

4. Opensees capabilities in the numerical analysis

The Open System for Earthquake Engineering Simulation (Opensees) is a software framework for simulating the seismic response of structural and geotechnical system. It has advanced capabilities for modeling and analyzing the nonlinear response of systems using a wide range of material models, elements, and solution algorithms [5-7]. There will be discussed some important point of Opensees facilities which be implemented in this study.

4.1. Displacement-based beam-column element

This element is one dimensional element type based on the displacement formulation and considers the spread of plasticity along the element. The integration point needs to be determined in making section curvature interpolation along the element, so that the approximate displacement field of element nodes can be determined, the illustration can be seen at Fig. 5. The default integration type based on Gauss-Legendre, the others integration type available to be used for example Lobotto, Radau, Newtoncotes, and Trapezoidal.

4.2. Fiber section

Fiber section is composed of fibers, which containing a uniaxial material, an area, and local coordinate. It has several commands to built fiber section they are fiber to build single fiber, patch to build a number of fibers over a

geometric cross section, and layer to build a row of fibers along arch geometric. The convergence stress and strain distribution of uniaxial material depends on the degree of refining mesh along this section.

4.3. P-Delta transformation

During defining the element geometric transformation need to be determined incase making transformation beam element stiffness and resisting force from the basic system to the global coordinate system. There are three types of geometric transformation including Linear Transformation which performs a linear geometric transformation, P-Delta Transformation which performs a linear geometric transformation considering second order P-Delta effects, and Corotational Transformation which performs an exact geometric transformation.

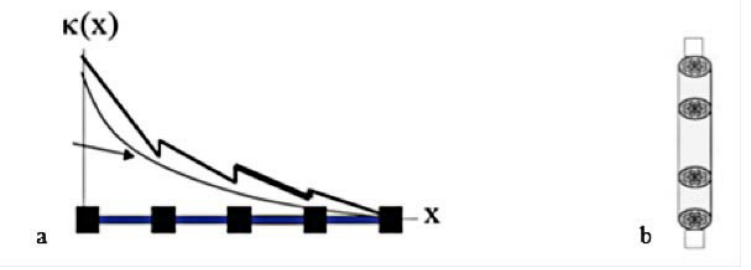

Fig. 5. (a) Curvature interpolation of displacement-based beam-column element [9]; (b) integration point of displacement-based beam-column element with fiber section[9].

5. Numerical analysis

5.1. Structure idealization

The RC column accompanied with FDM to be idealized as frame element in the two dimensional model with three degree of freedom. The selecting element type needs to consider based on the specimen set up condition. The upper end of middle column is idealized as elastic frame in case to be used as loading point support that should has elastic behavior. The other hand the Displacement-based Beam-column Element with fiber section is applied to the other column elements. The important things of this are the integration point number of frame element and also the division number of fiber section. Those parameters touch convergence degree in the numerical analysis, which the implementation can be seen at Fig. 6.

The friction devices are supposed as Two Node Link Element with Steel01 Material in the parallel direction and elastic material properties in the perpendicular direction of those. The material parameter will be discussed in sub section of friction devices parameter bellow.

5.2. Concrete material parameter

The concrete constitutive material implements Concrete02 Material adopts Kent-Park modified by Scott concept. The cover concrete has peak stress 37.00 MPa at the strain 0.002 and zero ultimate stress at ultimate strain 0.00429, otherwise incase confinement effect of transversal reinforcement the core concrete has peak stress 41.50 MPa at the strain 0.00224 and ultimate stress 8.30 MPa at ultimate strain 0.06365, the illustration can be seen at Fig. 7.

5.3. Steel material parameter

The reinforcing steel material utilizes to the Steel02 Material based on the Giufre-Menegotto-Pinto theory. The input parameter contains f_y is yield strength, E is elastic modulus, b is hardening ratio, and the parameter to control

the transition between elastic to plastic branches that are R_0, cR_1, and cR_2. The steel material input parameter can be seen at Table 3.

5.4. Friction devices parameter

The friction devices to be idealized as elastic-plastic material, the elastic condition reflects the sliding has not yet occurred, otherwise plastic condition shows the sliding has occurred. The Steel01 Material is used for this study that to construct a uniaxial bilinear steel material with kinematic hardening and optional isotropic hardening based on the Fedeas [8,9].

The friction coefficient value to be assumed 0.5 with hardening ratio is 0.0005 and the sliding displacement starts from 0.025 mm, those values based on the some trials of the numerical analysis. The example input parameter of friction devices with Steel01 Material for case T10 can be seen at Table 4.

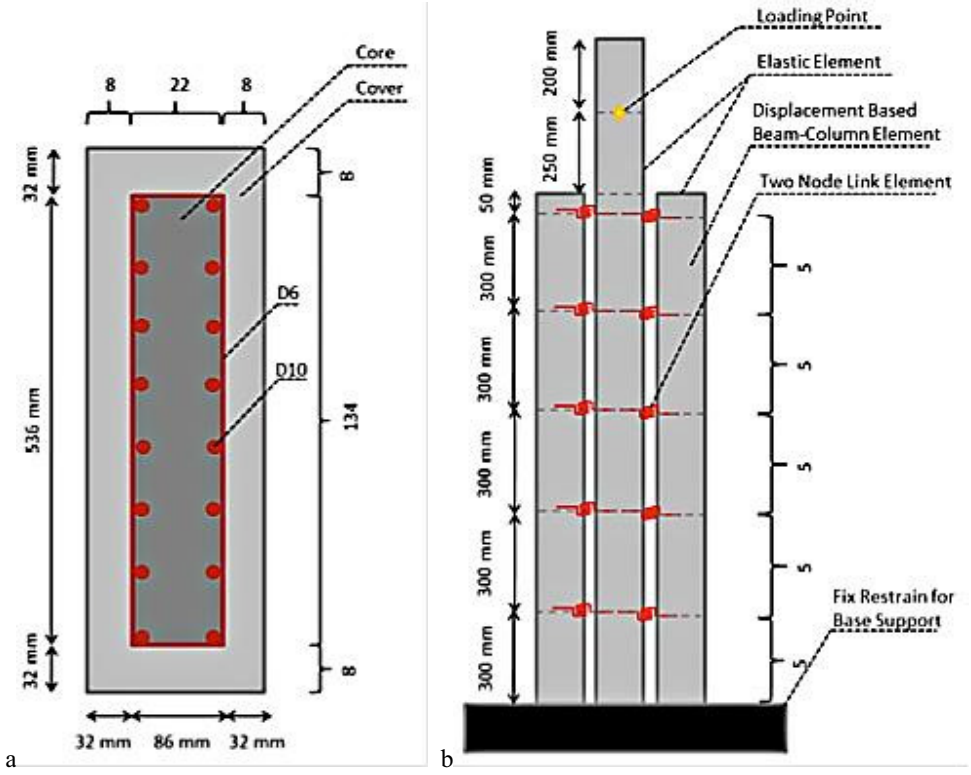

Fig. 6. (a) Fiber section of RC column idealization; (b) RC column accompanied with FDM structure idealization.

Table 3. Longitudinal reinforcing steel constitutive material input parameter.

f_y (MPa)	E (MPa)	B	R_0	cR_1	cR_2
345	200000	0.05	19.5	0.925	0.5

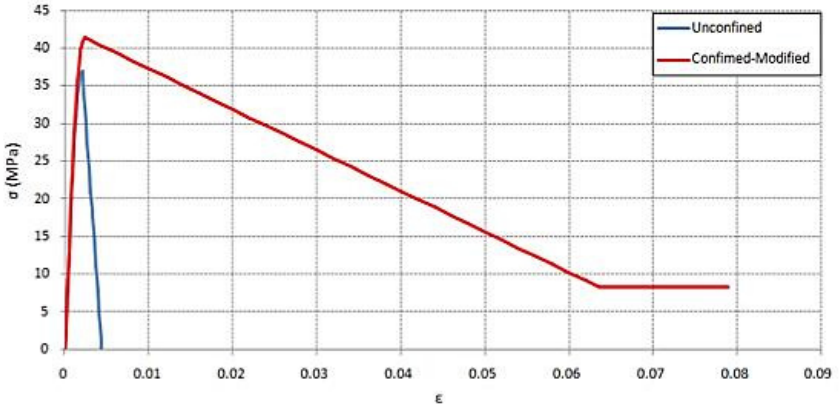

Fig. 7. Concrete constitutive material.

Table 4. The parameters input of friction devices case T10.

Confinement force (KN)	*fy* (KN)	*E* (KN)	*b*
100.0	50.0	2000	0.0005
75	37.5	1500	0.0005
50	25.0	1000	0.0005
25	12.5	500	0.0005
0.0	0.0	0.0	0.0005

6. Result

The numerical analysis result discusses about hysteresis curves of the structures under cyclic loading, curvature distribution of the columns member, and force displacement relation of friction devices. Fig. 8 up to Fig. 11 are hysteresis curves on the remaining elastic behavior, Fig. 12 and Fig.13 are hysteresis curves on the elastic up to the plastic behavior, Fig. 12 and Fig.13 are curvature distribution curve of columns member, Fig.14 and Fig.15 are force and displacement relation curve of friction devices.

6.1. The Hysteresis curve of the structure

Based on the hysteresis curves under all elastic behaviors the numerical analysis result has similarities in the terms of separated stiffness (K_s), unloading stiffness and peak force value at each loading cycle. The other hand the numerical analysis result has greater value than experiment result in the term monolith stiffness (K_m) at the early loading and reloading. Those differences of monolith stiffness probably occur because the specimens have been applied previous cyclic loading history.

Referring to the observation reached plastic behavior in both case T20-3 and T40 the numerical analysis results have similarities in the terms of separated stiffness (K_s) and unloading stiffness. However in T20-3 case the numerical analysis result has greater loading and reloading stiffness value than the experiment result, instead the peak force value of numerical analysis occurs less than experiment. And the other hand in T40 case the numerical analysis result has greater of all peak force value, loading and reloading stiffness than the experiment result. Those differences occur probably due to in the large deformation the friction devices did not perform as ideal condition, the contact action between the friction materials surfaces did not work properly. In the T20-3 case the numerical analysis result has less peak force value then the experiment result, instead in the T40 case the numerical analysis result has larger peak force value then the experiment result. This anomaly occurs probably due to the difference the

bolt placement method between specimen 1 and specimen 2, the difference also can be observed back on Nakamura's research [1].

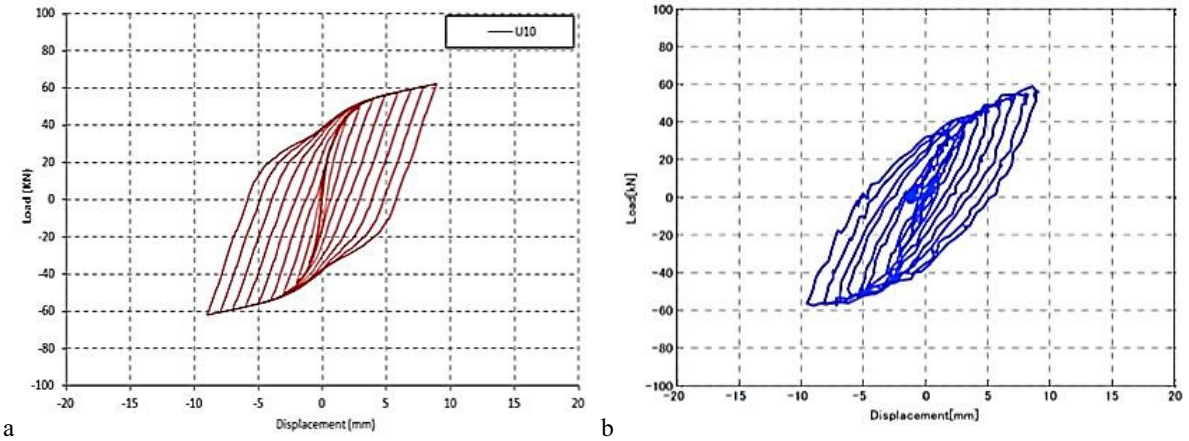

a b

Fig. 8. (a) Numerical result of U10 hysteresis loop; (b) experiment result of U10 hysteresis loop.

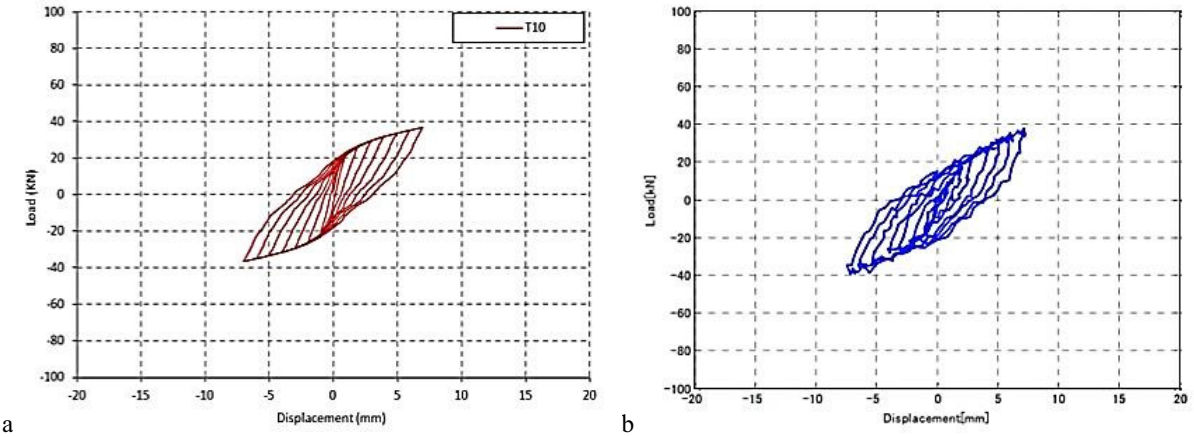

a b

Fig. 9. (a) Numerical result of T10 hysteresis loop; (b) experiment result of T10 hysteresis loop

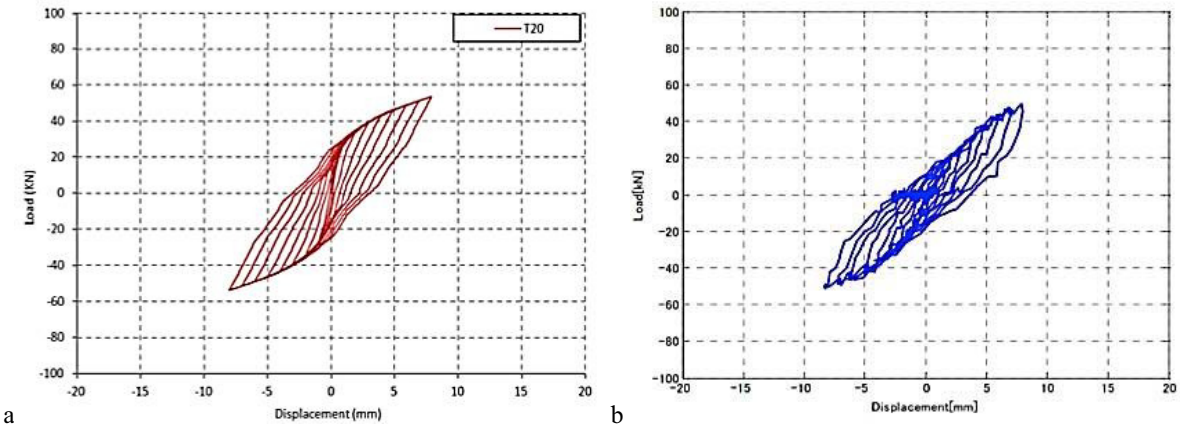

Fig. 10. (a) Numerical result of T20 hysteresis loop; (b) experiment result of T20 hysteresis loop

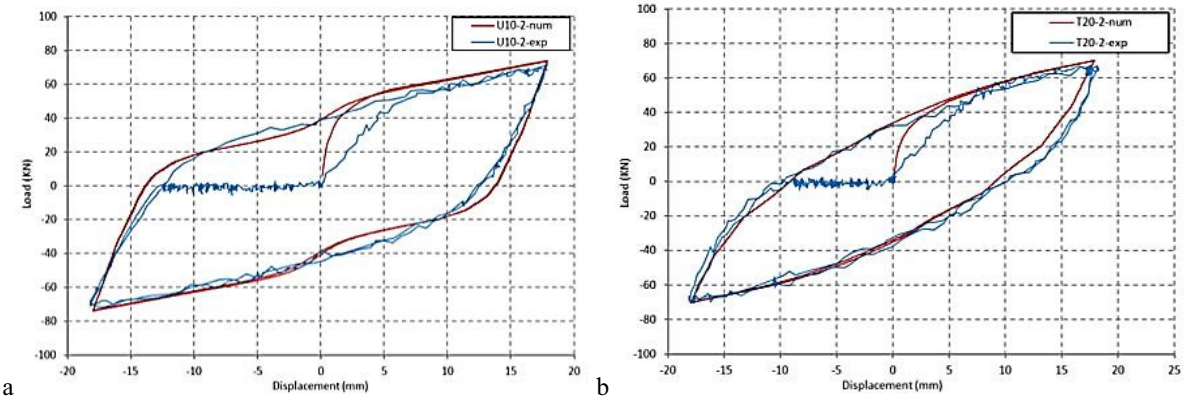

Fig. 11. (a) Numerical and experiment comparison of U10-2 hysteresis loop; (b) numerical and experiment comparison of T20-2 hysteresis loop

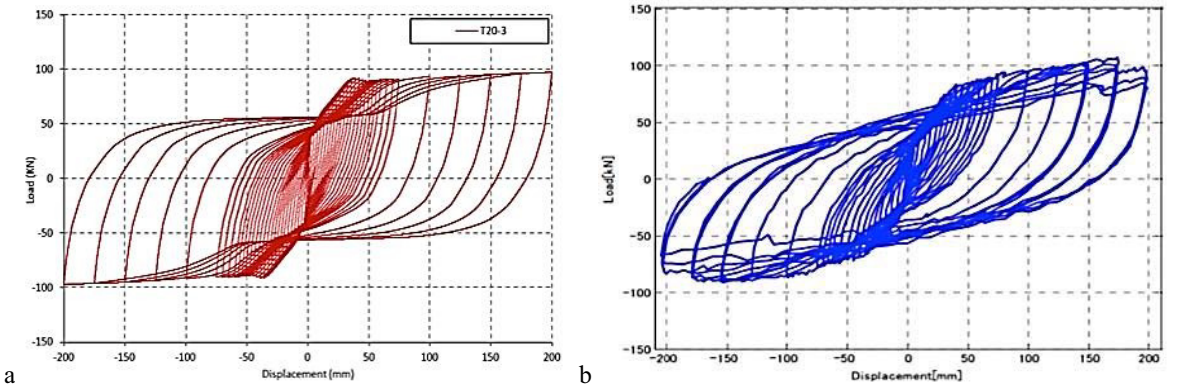

Fig. 12. (a) Numerical result of T20-3 hysteresis loop; (b) experiment result of T20-3 hysteresis loop

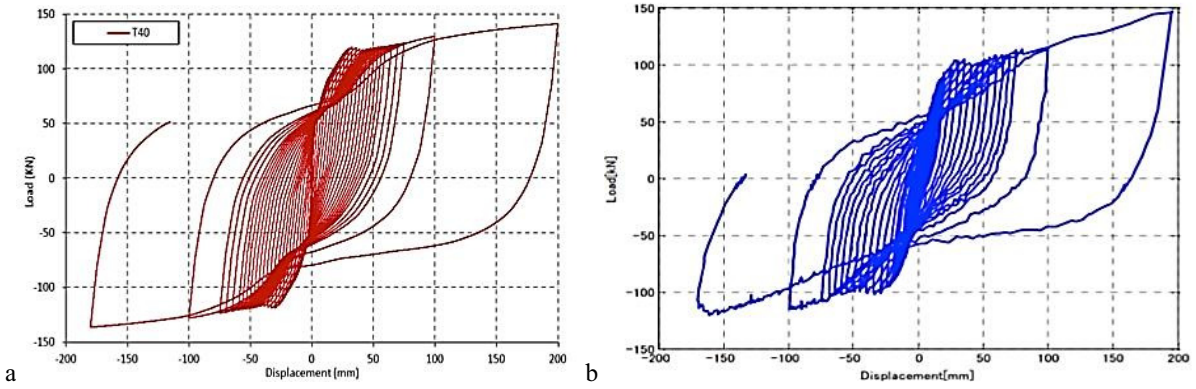

a b

Fig.13. (a) Numerical result of T20-3 hysteresis loop; (b) experiment result of T20-3 hysteresis

6.2. Curvature distribution

The curvature of columns that to be monitored in the maximum displacement of U10-2 and T20-2 scenarios show that the numerical results have same curvature distribution pattern, however the numerical analysis results have adjacent curvature value in each other of columns instead the experiment result, the graph can be seen at Fig.15. Those curvatures differences between numerical result and experiment result probably because the connection idealization of friction devices and PC bolts in the model are not fully able be realized like the laboratory specimens condition.

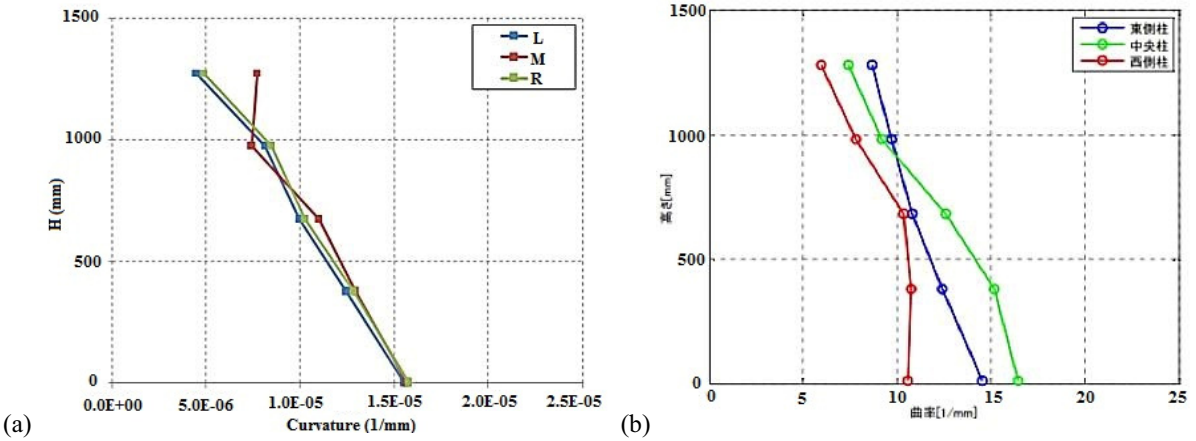

(a) (b)

Fig.14. (a) Numerical result of U10-2 curvature distribution; (b) experiment result of U10-2 curvature distribution

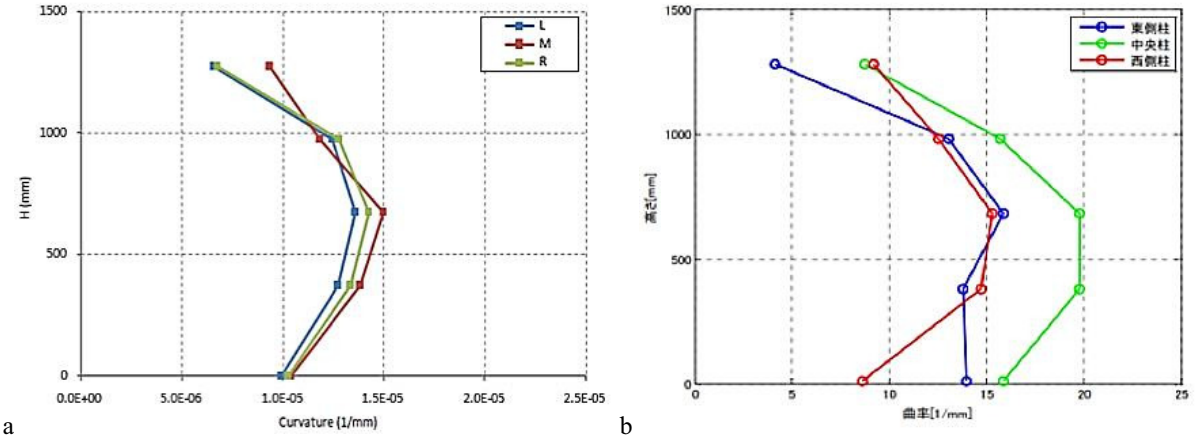

Fig.15. (a) Numerical result of T20-2 curvature distribution; (b) experiment result of T20-2 curvature distribution

6.3. Friction devices force and displacement characteristic

The force and displacement monitoring of friction devices be done in this numerical study to record the friction devices work at difference confinement distribution. Therefore, this comparison between U10-2 and T20-2 are selected at displacement 3 mm to monitor sliding rate of friction each devices and full cyclic loading to monitor the maximum sliding displacement.

Based on the Fig. 16 the bottom friction device of U10-2 case has larger sliding rate then T20-2 case, instead the second bottom up to the top of friction devices of U10-2 case have larger sliding rate then T20-2 case. Show that averagely the column with triangle confinement distribution has larger sliding rate than column with uniform confinement distribution.

Based on the Fig. 17 the bottom until second bottom number of friction device of U10-2 case has larger sliding displacement then T20-2 case, instead the forth bottom up to the top of friction devices of U10-2 case have less sliding displacement then T20-2 case. Show that the column with uniform confinement distribution has small displacement variation from bottom to top location than column with triangle confinement distribution.

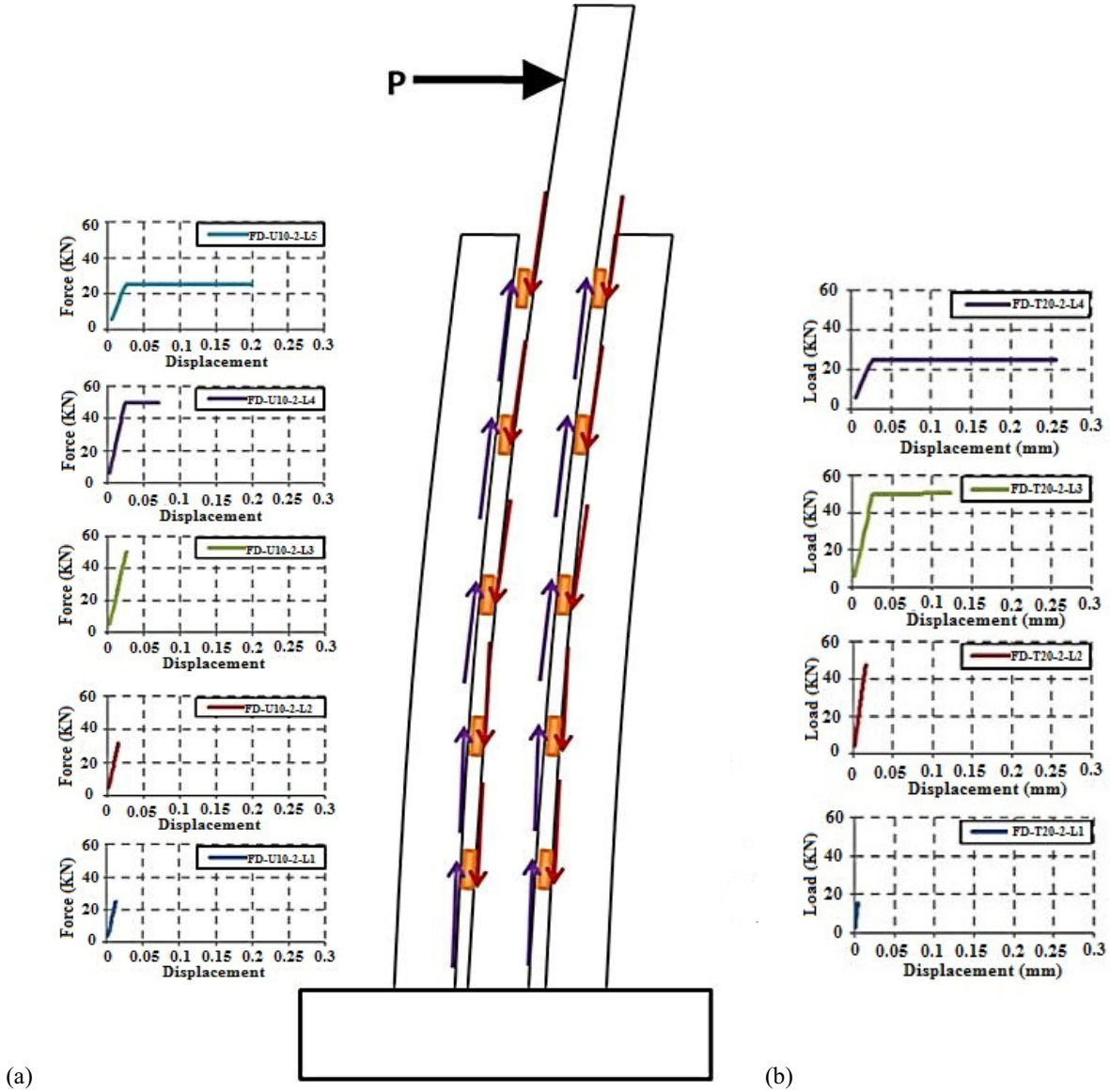

Fig. 16. The force and displacement relation of the friction devices with configuration at 3 mm drift (a) U10-2; (b) T20-2.

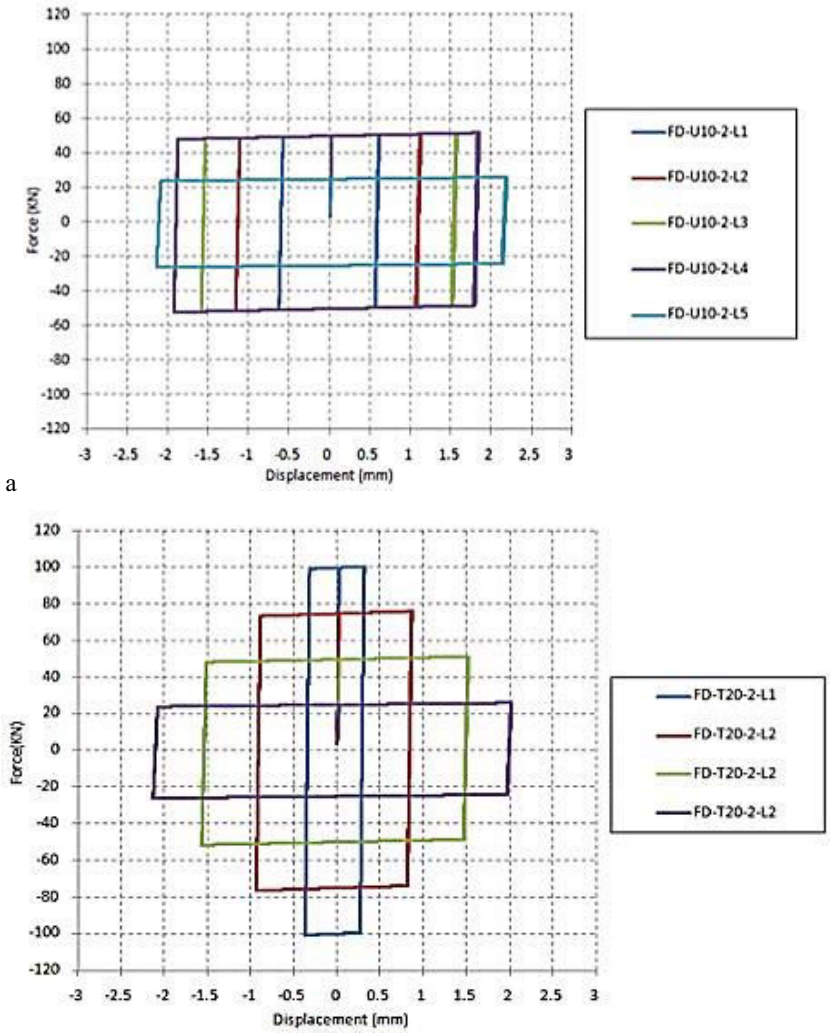

Fig. 17. The force and displacement relation of the friction devices with configuration (a) U10-2; (b) T20-2

7. Conclusion

The numerical analysis with fiber model is success to simulate the experiment of column accompanied with FDM under cyclic loading, by determining the appropriate constitutive materials parameters of friction device, concrete, and reinforcing steel. The comparison results can be seen at hysteresis curve and curvature distribution that have enough satisfied result for numerical simulation study.

Some difference result between numerical analysis and experiment occur due to previous cyclic loading history related to the monolith stiffness, probably lack of precision the friction devices due to large deformation and the difference confinement method related the plastic condition, and the inability to idealize the friction devices and PC bolts as the specimen condition related to the curvature distribution.

The force and displacement monitoring are useful to know the confinement distribution role the slip distribution to each friction devices. In the small deformation of this structure the uniform distribution of confinement has slower sliding rate than triangle distribution, however in the service deformation of this structure the uniform distribution has small displacement variation from bottom to top location than triangle confinement distribution.

8. Improvement

Some optimization methods like using SNOPT need to be used in fitting the hysteresis curve task.

References

[1] Nakamura, “The Elasto-Plastic Behavior of the Rectangular RC Column Accompanied with Friction Damping Mechanism with Complex Confinement ”. Graduate Thesis, Kyoto University, 2011.
[2] Nakamura,Takahashi, and Sawada “The Elasto-Plastic Behavior of the Rectangular RC Column Accompanied with Friction Damping Mechanism .”JSCE A1, Vol. 68, No. 4, 2012.
[3] Nakamura, “The Study on Earthquake Response Mechanism of Set RC Columns with Unity of 13 Frictional Damping Mechanism”. Master Thesis,Kyoto University, 2013.
[4] Pall, A.S., Marsh, C. “Energy Dissipation in Large Panel Structures Using Limited Slip Bolted Joints”, AICAP/CEB Seismic Conference, Rome, Italy, 1979, 3:27-34.
[5] Mazzoni, McKenna, Scott, and Fenves, “Opensees Command Language Manual.”, 2007.
[6] McKenna, Scott, and Fenves, “Nonlinear Finite-Element Analysis Software Architecture Using Object of Composition.”ASCE, USA, 2010.
[7] Vezna Terzic, “Forced-base Element vs. Displacement-based Element”.Opensees, UC Barkeley,2011.
[8] Morales and Tirca, “Numerical Simulation and Design of Friction-Damped Steel of Frame Structures.”, 15 WCEE, Lisboa, 2012.
[9] Morales, “Numerical Simulation of Steel Frames Equipped with Frictional-Damped-Diagonal-Bracing Devices.”, Master Thesis, Canada, 2011.